Nonintegrable Floquet Ising model with duality twisted boundary conditions

Aditi Mitra,[1,2] Hsiu-Chung Yeh,[1] Fei Yan,[3] and Achim Rosch[2]
[1]*Center for Quantum Phenomena, Department of Physics, New York University, 726 Broadway, New York, New York 10003, USA*
[2]*Institute for Theoretical Physics, University of Cologne, 50937 Cologne, Germany*
[3]*NHETC and Department of Physics and Astronomy, Rutgers University, 136 Frelinghuysen Road, Piscataway, New Jersey 08854, USA*

(Received 11 April 2023; revised 7 June 2023; accepted 8 June 2023; published 14 June 2023)

Results are presented for a Floquet Ising chain with duality twisted boundary conditions, taking into account the role of weak integrability breaking in the form of four-fermion interactions. In the integrable case, a single isolated Majorana zero mode exists which is a symmetry in the sense that it commutes both with the Floquet unitary and the Z_2 symmetry of the Floquet unitary. When integrability is weakly broken, both in a manner so as to preserve or break the Z_2 symmetry, the Majorana zero mode is still found to be conserved for small system sizes. This is reflected in the dynamics of an infinite-temperature autocorrelation function which, after an initial transient that is controlled by the strength of the integrability breaking term, approaches a plateau that does not decay with time. The height of the plateau agrees with a numerically constructed conserved quantity and is found to decrease with increasing system sizes. It is argued that the existence of the plateau and its vanishing for larger system sizes is closely related to a localization-delocalization transition in Fock space triggered by the integrability-breaking interactions.

DOI: 10.1103/PhysRevB.107.245416

I. INTRODUCTION

The transverse-field Ising model is one of the most basic models for understanding fundamental concepts in condensed matter physics such as phase transitions, topological order, non-Abelian excitations, and duality. The famous Kramers-Wannier duality transformation [1] maps the Ising model to its dual, where the dual is also an Ising model but with the couplings, corresponding to the Ising exchange interactions and the transverse fields, interchanged. At the level of wave functions, the duality transformation maps the doubly degenerate ferromagnetic ground state to the nondegenerate paramagnetic ground state. Since this is a two-to-one mapping, the duality transformation, when represented as an operator, is a noninvertible operator [2,3].

The duality transformation can be implemented through a duality defect, which has some remarkable topological properties, namely, that it locally commutes with the transfer matrix of the corresponding two-dimensional classical model or the generator of time evolution in the quantum (1+1)-dimensional (D) model [2–4]. In fact, the transverse-field Ising model hosts two topological defects, i.e., one is related to the Z_2 or spin-flip symmetry ($\mathcal{D}_\psi$) and the other performs the duality transformation ($\mathcal{D}_\sigma$). These topological defects obey the Ising anyon fusion rules $\mathcal{D}_\sigma^2 = \mathcal{I} + \mathcal{D}_\psi$, $\mathcal{D}_\psi \mathcal{D}_\sigma = \mathcal{D}_\sigma \mathcal{D}_\psi = \mathcal{D}_\sigma$, $\mathcal{D}_\psi^2 = \mathcal{I}$, with $\mathcal{I}$ representing the identity operator. These topological defects, while traditionally studied in the context of ground-state properties and/or in the context of conformal field theories [5–9], can in fact be constructed on the lattice [2,3]. Moreover, this construction can also be generalized to the Floquet version of the Ising model [10]. It has also been shown how to implement the duality transformation using gates and measurements [11,12], where, depending on the measurement outcome, four different kinds of Kramers-Wannier duality transformations may be identified [12].

Topological defects can also generate nontrivial boundary conditions in the system [2,7,13–18]. Consider a (1+1)-D system placed on a spatially circular chain; a timelike spin-flip defect corresponds to imposing antiperiodic boundary conditions along the circular chain. Similarly, a timelike duality defect corresponds to imposing duality twisted boundary conditions. Recently, the integrable Floquet Ising model with duality twisted boundary conditions was studied [10]. It was shown that the duality twist allows the chain to host a single isolated Majorana zero mode (rather than a pair of Majorana zero modes), despite the Floquet driving. This mode was detected in two ways. The first was by the full analytic construction of the Majorana operator, and the second was by numerically studying the autocorrelation function of a local operator that has an overlap with the Majorana mode. It is noteworthy that the Majorana zero mode that exists in the presence of a duality twist does not lead to any degeneracy or pairing of the eigenspectra of the Floquet unitary, in contrast to Majorana modes (also known as strong modes) that appear with open boundary conditions [19–21]. In this paper, we discuss the effects of weak integrability breaking terms on the duality twisted Floquet Ising chain.

The paper is organized as follows. In Sec. II, we review some of the properties of the integrable Floquet Ising model with a duality twist. We also present results such as the effect of translating the duality twist along the integrable Floquet chain, and we highlight some subtleties of the dynamics of the Majorana operators. In Sec. III, we present results for the nonintegrable Floquet Ising model, showing how the Majorana mode is still remarkably stable for finite system sizes. In Sec. IV, we present a phenomenological argument

for the stability of the Majorana zero mode. We present our conclusions in Sec. V.

II. INTEGRABLE FLOQUET ISING MODEL WITH A DUALITY TWIST

Let us consider a chain with $2L$ sites labeled by $0, 1, 2 \ldots 2L-1$. The spins reside on the odd sites $1, 3, \ldots 2L-1$, while the even sites are empty (and can be considered to be dual sites) [2,10]. We impose periodic boundary conditions where site n is the same as site $2L+n$. We denote X_j, Y_j, Z_j as the Pauli operators on site j. The usual defectless and integrable Floquet Ising unitary, allowing for spatially inhomogeneous couplings, is

$$U = \left[\prod_{j=0}^{L-1} W^X_{2j+1}(u_{2j+1})\right]\left[\prod_{j=0}^{L-1} W^{ZZ}_{2j}(u_{2j})\right], \tag{1}$$

where

$$W^X_{2j+1}(u_{2j+1}) = e^{-iu_{2j+1}X_{2j+1}}, \tag{2a}$$

$$W^{ZZ}_{2j}(u_{2j}) = e^{-iu_{2j}Z_{2j-1}Z_{2j+1}}. \tag{2b}$$

Above, $W^X_{2j+1}(u_{2j+1})$ represents the single-site unitary gate that corresponds to applying a transverse field of strength u_{2j+1} along X on the spin at site $2j+1$. $W^{ZZ}_j(u_{2j})$ is the two-site unitary gate that corresponds to a ZZ-type Ising interaction of strength u_{2j} between spins at sites $2j-1$ and $2j+1$. The above unitary has a discrete Z_2 symmetry generated by

$$D_\psi = X_1 X_3 \ldots X_{2L-1}, \tag{3}$$

which describes the simultaneous flip of all spins. While for the defectless case presented above, u_{even} corresponds to Ising interactions while u_{odd} corresponds to the strength of the transverse field, we will show later that a duality defect will interchange the role of the two couplings.

The duality twisted boundary conditions on the $2L-2$ link, i.e., the link between sites $2L-3, 2L-1$, corresponds to [2,10] removing the transverse field at site $2L-1$, and changing the Ising coupling between sites $2L-3$ and $2L-1$ from $Z_{2L-3}Z_{2L-1}$ to a mixed Ising coupling, $Z_{2L-3}X_{2L-1}$. This is shown in the top left panel of Fig. 1 for $L=6$. Thus, the Floquet unitary with a duality twist between sites $2L-3$ and $2L-1$ is

$$T_{\sigma,2L-1} = \left[\prod_{j=0}^{L-2} W^X_{2j+1}(u_{2j+1})\right] e^{-iu_{2L-2}Z_{2L-3}X_{2L-1}} \times \left[\prod_{j=0}^{L-2} W^{ZZ}_{2j}(u_{2j})\right]. \tag{4}$$

In particular, u_{2L-2} controls the strength of the exchange interaction, albeit of the mixed coupling type ZX. Moreover, u_{2L-1} is missing due to the absence of the transverse field on site $2L-1$. The symmetry operator in the presence of the duality twist is no longer D_ψ but Ω, where

$$\Omega = iZ_{2L-1}D_\psi = -(X_1 \ldots X_{2L-3})Y_{2L-1}. \tag{5}$$

We will show later that unitary transformations that shift the location of the duality defect will locally (along the trajectory of the shifted defect) interchange the role of the couplings $u_{\text{even}}(u_{\text{odd}})$ from an Ising (transverse-field) coupling to a transverse-field (Ising) coupling.

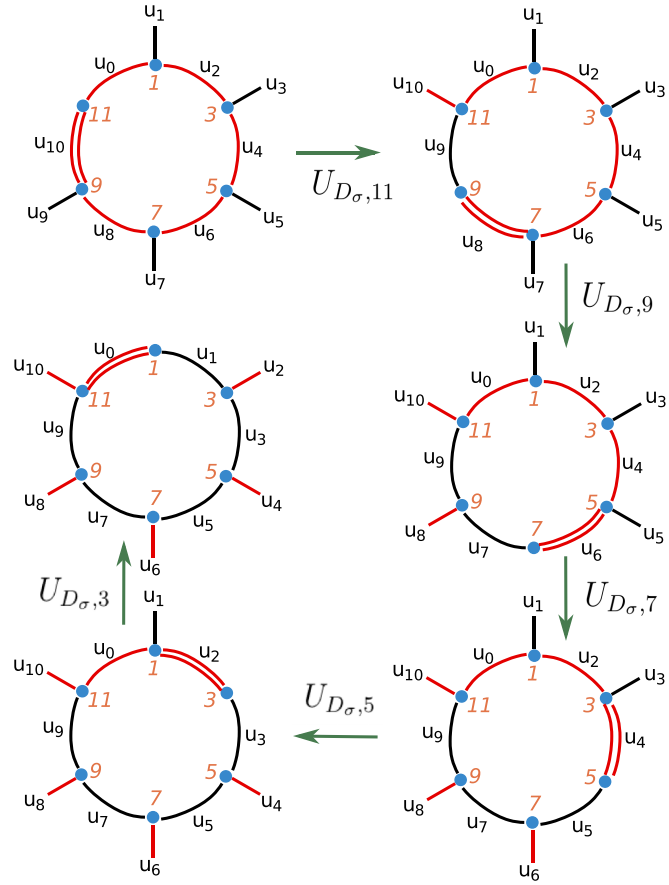

FIG. 1. Duality twist and its translation for $L=6$. Top left: Initial configuration where a duality twist (double red line) exists between sites 9 and 11, where the mixed coupling term is $u_{10}Z_9X_{11}$. All the odd couplings (black) correspond to transverse fields ($u_{2j+1}X_{2j+1}$, $j \neq 5$), while all the even couplings (red) are Ising exchange interactions ($u_{2j}Z_{2j-1}Z_{2j+1}$, $j \neq 5$). A Majorana zero mode is localized around site 11. Top right: The twist has been moved to the neighboring link, i.e., between sites 7 and 9. In this process, a domain wall is introduced at site 11 where u_9, u_{10} exchange roles. The Majorana continues to reside around site 11. Other panels: Further translations of the duality twist do not move the Majorana zero mode. Meanwhile, the Kramers-Wannier transformation is applied to the region between the duality twist and the domain wall, interchanging the roles of u_{even} and u_{odd}.

The duality twisted boundary condition is a highly nonlocal perturbation in the language of Majorana fermions. In order to show this, we rewrite the Floquet unitary in terms of the Majorana fermions,

$$\gamma_{2j} = \left(\prod_{k=-1}^{j-1} X_{2k+1}\right) Z_{2j+1}, \quad j = 0, \ldots, L-2, \tag{6a}$$

$$\gamma_{2j+1} = -\left(\prod_{k=-1}^{j-1} X_{2k+1}\right) Y_{2j+1}, \quad j = 0, \ldots, L-2, \tag{6b}$$

$$\gamma_{2L-2} = Z_{2L-1}, \quad \gamma_{2L-1} = -Y_{2L-1}. \tag{6c}$$

The Majorana fermions are constructed using Pauli strings that start from site $2L-1$ which hosts the mixed coupling term. Thus, only the Majorana fermions at site $2L-1$ are defined without a Pauli string. The Majorana fermions satisfy the usual anticommutation relations $\{\gamma_{2j},\gamma_{2k}\}=\{\gamma_{2j+1},\gamma_{2k+1}\}=2\delta_{kl}$ and $\{\gamma_{2j},\gamma_{2k+1}\}=0$. With these definitions, all the Majorana fermions can be shown to commute with the symmetry operator (5) except for γ_{2L-2} which anticommutes with it,

$$\Omega\gamma_{2L-2}=-\gamma_{2L-2}\Omega, \tag{7a}$$

$$\Omega\gamma_{2j}=\gamma_{2j}\Omega,\ j=0,\ldots,L-2, \tag{7b}$$

$$\Omega\gamma_{2j+1}=\gamma_{2j+1}\Omega,\ j=0,\ldots,L-1. \tag{7c}$$

From (6), it follows that

$$\begin{aligned}
&\gamma_0=[X_{2L-1}]Z_1,\ \ \gamma_1=-[X_{2L-1}]Y_1,\\
&\gamma_2=[X_{2L-1}X_1]Z_3,\ \ \gamma_3=-[X_{2L-1}X_1]Y_3,\\
&\gamma_4=[X_{2L-1}X_1X_3]Z_5,\ \ \gamma_5=-[X_{2L-1}X_1X_3]Y_5,\\
&\vdots\\
&\gamma_{2L-4}=[X_{2L-1}X_1X_3\ldots X_{2L-5}]Z_{2L-3},\\
&\gamma_{2L-3}=-[X_{2L-1}X_1X_3\ldots X_{2L-5}]Y_{2L-3}.
\end{aligned} \tag{8}$$

Substituting the above in (5), one obtains $\Omega=[(-i)\gamma_0\gamma_1(-i)\gamma_2\gamma_3\ldots(-i)\gamma_{2L-4}\gamma_{2L-3}]\gamma_{2L-1}$. Thus, Ω contains an odd number of Majorana fermions, i.e., it contains all the Majoranas except γ_{2L-2}. The Floquet unitary (4) can now be written as

$$\begin{aligned}
T_{\sigma,2L-1}=&e^{-\sum_{j=0}^{L-2}u_{2j+1}\gamma_{2j}\gamma_{2j+1}}e^{-u_{2L-2}\Omega\gamma_{2L-3}\gamma_{2L-1}}\\
&\times e^{-\sum_{j=0}^{L-2}u_{2j}\gamma_{2j-1}\gamma_{2j}},
\end{aligned} \tag{9}$$

where the Majorana fermion γ_{2L-2} is noticeably absent in the Floquet unitary. Despite this, γ_{2L-2} does not commute with the Floquet unitary because of the presence of the symmetry operator Ω attached to the mixed coupling term, and because Ω anticommutes with γ_{2L-2}. Since all the remaining Majoranas commute with Ω, we can study the dynamics in a given eigensector of Ω, and, in this case, $T_{\sigma,2L-1}$ is entirely bilinear in Majorana fermions, and hence integrable.

In addition, the Floquet unitary has to have a determinant of 1, and given that the Floquet unitary contains an odd number of fermions, this implies it has to have a single unity eigenvalue, namely, a single Majorana zero mode. This mode commutes with the time evolution operator, while its "partner" γ_{2L-2} (the other Majorana operator which does not explicitly appear in $T_{\sigma,2L-1}$) does not. Depending on the coupling parameters, this Majorana zero mode could be delocalized, for example, at the self-dual point where $u_{2j+1}=u_{2j}=$ constant, or localized. It was shown that for uniform couplings $u_{2j+1}=gT/2$, $u_{2j}=JT/2$, the Majorana zero mode is localized at the duality twist, with a localization length of [10]

$$\xi\sim\left(\ln\left\{\frac{\tan[\max(g,J)]}{\tan[\min(g,J)]}\right\}\right)^{-1}. \tag{10}$$

For the sake of clarity, let us construct the Majorana zero mode for two limiting cases. The first case is when $u_{2j}=0$. In this case, the system only has transverse fields, and there are many conserved quantities corresponding to all the X_{2j+1}, as well as Y_{2L-1} and Z_{2L-1} due to the absent transverse field at site $2L-1$. In this case, the spectrum of the many-particle Floquet operator has degeneracies because we have the following operator algebra: $[T_{\sigma,2L-1},\Omega]=0$, $[T_{\sigma,2L-1},Z_{2L-1}]=0$ and $\{\Omega,Z_{2L-1}\}=0$. Thus the operator Z_{2L-1}, when acting on the $\Omega=1$ eigenstate with a given quasienergy, changes it to the $\Omega=-1$ eigenstate with the same quasienergy. When an infinitesimal Ising interaction is switched on, only one zero mode survives, which has the largest overlap with Y_{2L-1} (i.e., γ_{2L-1}). This zero mode commutes rather than anticommutes with Ω and therefore does not imply a degeneracy of the Floquet spectrum. In general, in contrast to open boundary conditions [19–21], the degeneracy of the many-particle Floquet spectrum with a duality twist does not survive for generic couplings [10]. However, in the high-frequency limit, a Kramers' degeneracy does emerge [2].

The second limiting case is when all the transverse fields are zero $u_{2j+1}=0$, while all the exchange interactions are uniform and equal, $u_{2j}=u$. For this case, the Majorana zero mode is [10]

$$\begin{aligned}
\Psi&=\frac{1}{\sqrt{1+\sec^2 u}}[\Omega\gamma_{2L-3}+\tan u\,\gamma_{2L-1}+\gamma_0]\\
&=\frac{1}{\sqrt{1+\sec^2 u}}[Z_{2L-3}Z_{2L-1}-\tan u Y_{2L-1}+X_{2L-1}Z_1].
\end{aligned} \tag{11}$$

Deviations from this fine-tuned point do not change the fact that the single site operator $Y_{2L-1}=-\gamma_{2L-1}$ has an overlap with the Majorana zero mode. In later sections, we will use the autocorrelation function of Y_{2L-1} to numerically detect the Majorana zero mode.

A. Spatial translation of the duality twist

We now show that a unitary transformation can move the duality defect (or twist) from one link to another, and in doing so, the role of u_{even} and u_{odd} is interchanged, introducing a "domain wall" in the space of coupling parameters.

In what follows, starting with a duality twist located in between the sites $2L-3, 2L-1$ [corresponding to the unitary (4)], we will perform a unitary transformation which moves the duality twist to the link between sites $2L-5, 2L-3$. In particular, before the action of the unitary transformation, there was no magnetic field at site $2L-1$ and there were exchange terms of the kind $Z_{2L-3}X_{2L-1}$, $Z_{2L-5}Z_{2L-3}$. The unitary transformation will remove the magnetic field on site $2L-3$, while reintroducing a magnetic field on site $2L-1$. In addition, the unitary transformation will change the exchange terms to $Z_{2L-5}X_{2L-3}$ and $Z_{2L-3}Z_{2L-1}$. The couplings on all other sites will remain unchanged.

In order to achieve this, let us define the controlled-Z (CZ) gate,

$$\text{CZ}_{1,2}=|0\rangle\langle 0|_1\otimes 1_2+|1\rangle\langle 1|_1\otimes Z_2. \tag{12}$$

We will now show that the unitary transformation [2],

$$U_{D_\sigma,2L-1}=\text{CZ}_{2L-3,2L-1}H_{2L-3}, \tag{13}$$

will implement the required transformation where $H_j=(X_j+Z_j)/\sqrt{2}$ is the Hadamard gate on site j.

First note that the action of the CZ gate on the unitary in (4) is

$$\begin{aligned}\mathrm{CZ}^{\dagger}_{2L-3,2L-1}[T_{\sigma,2L-1}]\mathrm{CZ}_{2L-3,2L-1} &= \left[\prod_{j=0}^{L-3} W^{X}_{2j+1}(u_{2j+1})\right] \\ &\times e^{-iu_{2L-3}X_{2L-3}Z_{2L-1}} e^{-iu_{2L-2}X_{2L-1}} \left[\prod_{j=0}^{L-2} W^{ZZ}_{2j}(u_{2j})\right]. \quad (14)\end{aligned}$$

In particular, the transformations $X_{2L-3} \to X_{2L-3}Z_{2L-1}$ and $Z_{2L-3}X_{2L-1} \to X_{2L-1}$ have been implemented. At the next step, the Hadamard gate transforms $X_{2L-3}(Z_{2L-3})$ to $Z_{2L-3}(X_{2L-3})$, giving the transformed unitary

$$\begin{aligned}T'_{\sigma,2L-1} &= U^{\dagger}_{D_\sigma,2L-1} T_{\sigma,2L-1} U_{D_\sigma,2L-1} \\ &= \left\{\left[\prod_{j=0}^{L-3} W^{X}_{2j+1}(u_{2j+1})\right] \right. \\ &\times e^{-iu_{2L-3}Z_{2L-3}Z_{2L-1}} e^{-iu_{2L-4}Z_{2L-5}X_{2L-3}} e^{-iu_{2L-2}X_{2L-1}} \\ &\left. \times \left[\prod_{j=0}^{L-3} W^{ZZ}_{2j}(u_{2j})\right]\right\}. \quad (15)\end{aligned}$$

This realizes what we set out to do. In particular, after the unitary transformation, there is no magnetic field on site $2L-3$, a magnetic field on all other sites, and a $Z_{2L-5}X_{2L-3}$ twist. Note that the translation of the twist has locally interchanged an Ising coupling with a transverse-field coupling. This is reflected in u_{2L-2} now representing a transverse-field coupling, while u_{2L-3} becomes an Ising coupling. Now let us explore what happens to the symmetry Ω in (5). It is straightforward to see that

$$U^{\dagger}_{D_\sigma,2L-1}\Omega U_{D_\sigma,2L-1} = iZ_{2L-3}D_\psi. \quad (16)$$

To move the twist further to the link between sites $2L-7, 2L-5$, we need to apply

$$U_{D_\sigma,2L-3} = \mathrm{CZ}_{2L-5,2L-3}H_{2L-5}. \quad (17)$$

The above CZ gate will convert $Z_{2L-5}X_{2L-3} \to X_{2L-3}$ and $X_{2L-5} \to X_{2L-5}Z_{2L-3}$. After application of the Hadamard gate on site $2L-5$, one obtains the new unitary

$$\begin{aligned}T''_{\sigma,2L-1} &= U^{\dagger}_{D_\sigma,2L-3} T'_{\sigma,2L-1} U_{D_\sigma,2L-3} = \left\{\left[\prod_{j=0}^{L-4} W^{X}_{2j+1}(u_{2j+1})\right]\right. \\ &\times e^{-iu_{2L-3}Z_{2L-3}Z_{2L-1}} e^{-iu_{2L-5}Z_{2L-5}Z_{2L-3}} \\ &\times e^{-iu_{2L-6}Z_{2L-7}X_{2L-5}} e^{-iu_{2L-2}X_{2L-1}} e^{-iu_{2L-4}X_{2L-3}} \\ &\left. \times \left[\prod_{j=0}^{L-4} W^{ZZ}_{2j}(u_{2j})\right]\right\}. \quad (18)\end{aligned}$$

We now see that the u_{even} and u_{odd} have exchanged roles for two additional spins located on sites $2L-5, 2L-3$. Moreover, there is no transverse field on site $2L-5$.

Quite generally, the unitary transformation

$$U_{D_\sigma,2j+1} := \mathrm{CZ}_{2j-1,2j+1}H_{2j-1} \quad (19)$$

moves the duality link from between sites $2j-1, 2j+1$ to between sites $2j-3, 2j-1$. After this transition, what was originally a transverse-field coupling, u_{2j-1} becomes the Ising coupling between sites $2j-1$ and $2j+1$, while the original mixed coupling term u_{2j} becomes the transverse-field coupling for the spin at site $2j+1$. Denoting the term "domain wall" for the point where the Ising and transverse fields exchange roles, the very first translation introduces a domain wall and each subsequent translation increases the size of one "phase" relative to the other. This is highlighted pictorially in Fig. 1.

It should be noted that unitary transformations that move the duality twist have been constructed for the quantum Hamiltonian at the critical point [22], as well as for the classical 2D Ising system at and away from the critical point [2]. In this section, we have extended previous work by generalizing the unitary transformation to Floquet systems.

As we apply the unitary transformation to move the duality twist, the Majorana zero mode remains localized at the domain wall. To show this, we take as an example the exactly solvable case where all the transverse fields are zero and all the exchange interactions are equal. The zero mode is given in (11). After we move the duality twist from between sites $2L-3$ and $2L-1$ to between sites $2k-3$ and $2k-1$, the zero mode (expressed in spin degrees of freedom) gets transformed as

$$\begin{aligned}\Psi' &= U^{\dagger}_{D_\sigma,2k+1}\ldots U^{\dagger}_{D_\sigma,2L-1}\Psi U_{D_\sigma,2L-1}\ldots U_{D_\sigma,2k+1} \\ &= \frac{1}{\sqrt{1+\sec^2 u}}\left[-\tan u \prod_{j\geqslant k}^{L-1} X_{2j-1}Y_{2L-1}\right. \\ &\left. + \prod_{j\geqslant k}^{L-1} X_{2j-1}Z_{2L-1} + \prod_{j\geqslant k}^{L} X_{2j-1}Z_1\right]. \quad (20)\end{aligned}$$

In particular, the zero mode consists of string operators spanning between the duality twist and the domain wall at site $2L-1$. Our convention for the Jordan-Wigner transformation is such that Majorana fermions correspond to string operators attached to the duality twist. In terms of these Majorana fermions, the zero mode becomes

$$\Psi = \frac{1}{\sqrt{1+\sec^2 u}}[\gamma'_{2L-2} + \tan u\gamma'_{2L-1} + \gamma'_0], \quad (21)$$

where we denote the Majorana fermions as γ' to distinguish from the case where the duality twist is fixed to be between sites $2L-3$ and $2L-1$. The Majorana zero mode is indeed localized around the domain wall at site $2L-1$ and it remains there when one moves the location of the duality twist using the procedure described in Fig. 1.

For a different Floquet unitary from the one above, it was shown that when a domain wall exists, the Majorana mode is located at the domain wall [10]. In the ground state of a chain described by a time-independent Hamiltonian (equivalent to the high-frequency limit of the Floquet chain), a domain wall configuration of coupling constants would separate a paramagnetic phase from a ferromagnetic phase, with the Majorana

zero mode residing at the boundary of the two phases, i.e., at the domain wall [2]. In particular, the duality twist allows one to introduce an odd number of domain walls, unlike periodic boundary conditions which always require an even number of domain walls. In the Floquet context, while there is no phase, a Majorana mode nevertheless exists, localized at the domain wall across which $u_{\rm even}$, $u_{\rm odd}$ interchange roles.

B. Dynamics of γ_{2L-2}

The peculiarity of the duality twisted Floquet unitary in (9) is that while there are $2L$ Majorana fermions, only an odd number $(2L-1)$ of them appear explicitly, with the Majorana operator γ_{2L-2} absent from $T_{\sigma,2L-1}$. In addition, since all the Majorana fermions except γ_{2L-2} commute with the symmetry Ω, they transform in a standard manner in that they evolve into linear superpositions of single Majorana fermions. Denoting $\vec{\gamma} = [\gamma_0, \gamma_1, \gamma_2, \ldots, \gamma_{2L-3}, \gamma_{2L-1}]$ as a $2L-1$ component vector, this vector evolves as

$$T^\dagger_{\sigma,2L-1}\vec{\gamma}\,T_{\sigma,2L-1} = M_\Omega\vec{\gamma}, \tag{22}$$

where M_Ω is a $(2L-1)\times(2L-1)$ orthogonal matrix which depends on Ω. Thus, as long as one is interested in dynamics involving the above $2L-1$ Majorana fermions, the dynamics is integrable in that it scales linearly with system size L.

In contrast, the Majorana fermion γ_{2L-2}, due to its anticommutation with Ω, has a rather complicated time evolution given by [10]

$$\begin{aligned} T^\dagger_{\sigma,2L-1}&\gamma_{2L-2}T_{\sigma,2L-1} \\ &= \cos 2u_{2L-2}\gamma_{2L-2} \\ &\quad + \Omega\sin 2u_{2L-2}\cos 2u_0\gamma_{2L-2}\gamma_{2L-3}\gamma_{2L-1} \\ &\quad - \Omega\sin 2u_{2L-2}\sin 2u_0\gamma_{2L-2}\gamma_{2L-3}\gamma_0. \end{aligned} \tag{23}$$

Let us use the notation

$$[T^\dagger_{\sigma,2L-1}]^n\gamma_i(0)[T_{\sigma,2L-1}]^n = \gamma_i(n), \tag{24}$$

and define the operator

$$\begin{aligned} O = &[\cos 2u_{2L-2} - \Omega\sin 2u_{2L-2}\cos 2u_0\gamma_{2L-3}\gamma_{2L-1} \\ &+ \Omega\sin 2u_{2L-2}\sin 2u_0\gamma_{2L-3}\gamma_0], \end{aligned} \tag{25}$$

then,

$$T^\dagger_{\sigma,2L-1}\gamma_{2L-2}(0)T_{\sigma,2L-1} = \gamma_{2L-2}(0)O(0). \tag{26}$$

Thus, after two Floquet cycles,

$$(T^\dagger_{\sigma,2L-1})^2\gamma_{2L-2}(T_{\sigma,2L-1})^2 = \gamma_{2L-2}(0)O(0)O(1), \tag{27}$$

while after n Floquet periods,

$$\begin{aligned} &(T^\dagger_{\sigma,2L-1})^n\gamma_{2L-2}(T_{\sigma,2L-1})^n \\ &\quad = \gamma_{2L-2}(0)O(0)O(1)O(2)\ldots O(n-1). \end{aligned} \tag{28}$$

Thus, under Floquet time evolution, the γ_{2L-2} operator evolves into longer and longer strings of Majorana fermions. The dynamics is therefore nontrivial if it involves γ_{2L-2}. We may employ exact diagonalization (ED) to study how this Majorana evolves, and we will demonstrate its explicit time evolution in the subsequent sections. However, it is interesting to note that one gets a type of x-ray edge problem when calculating the time evolution of γ_{2L-2} because γ_{2L-2} takes $\Omega\to-\Omega$. In particular, we have

$$\begin{aligned} &(T^\dagger_{\sigma,2L-1})^n\gamma_{2L-2}(T_{\sigma,2L-1})^n \\ &\quad = \gamma_{2L-2}[T^\dagger_{\sigma,2L-1}(-\Omega)]^n[T_{\sigma,2L-1}(\Omega)]^n. \end{aligned} \tag{29}$$

In the above equation, the notation $T_{\sigma,2L-1}(\pm\Omega)$ keeps track of which Ω sector the unitary corresponds to.

III. NONINTEGRABLE DUALITY TWISTED UNITARY

In the remaining sections, we will study the system by performing ED on chains of length $L = 4, 6, 8, 10, 12, 14$. Since the sites are labeled as $0, 1, 2, \ldots 2L-1$ with the spins on the odd sites, the number of spins equals L. In addition, we will place the duality twist at the center of the chain, i.e., at $r = L-1 \in$ odd. Thus there is no transverse field on the spin at site r, and the exchange couplings between sites $r-2, r$ are of the mixed coupling type $Z_{r-2}X_r$. To keep the discussion simple, there will be no domain walls in the coupling configuration space. The Jordan-Wigner transformation starts from site r so that

$$\gamma_{r-1} = Z_r, \quad \gamma_r = -Y_r. \tag{30}$$

Thus, it is now Y_r that has an overlap with the zero mode, and it is Z_r that equals the Majorana fermion that does not explicitly enter the Floquet unitary. As before, periodic boundary conditions where $O_{2L+n} = O_{2L}$ are implied.

We choose all the nonzero transverse-field couplings to be uniform and equal to $gT/2$, and the ZZ and ZX Ising couplings are also chosen to be uniform and equal to $JT/2$. The discrete $\mathbb{Z}_2$ symmetry operator with the above labeling of sites is

$$\Omega = -X_1X_3\ldots X_{r-2}Y_rX_{r+2}\ldots X_{2L-1}. \tag{31}$$

We also break integrability by introducing a nearest-neighbor exchange interaction of the type $X_{2j-1}X_{2j+1}$, $j\in$ integer, which after a Jordan-Wigner transformation corresponds to four-fermion interactions. We consider two kinds of unitaries. One is $T_{\sigma,S}$, where the unitary still commutes with Ω. We achieve this by introducing XX interactions on all odd nearest-neighbor sites except between sites $r-2, r$ and $r, r+2$. The second unitary we consider is $T_{\sigma,A}$, where the XX type of exchange interaction exists between all odd nearest-neighbor sites, and therefore Ω is no longer a symmetry. Concretely, the unitary that preserves the Z_2 symmetry is

$$\begin{aligned} T_{\sigma,S} = &e^{-i(J_xT/2)\sum_{j\neq(r-1)/2,(r+1)/2,j=1}^{L}X_{2j-1}X_{2j+1}} \\ &\times e^{-i(gT/2)\sum_{j\neq(r-1)/2,j=1}^{L}X_{2j+1}} \\ &\times e^{-i(JT/2)Z_{r-2}X_r}e^{-i(JT/2)\sum_{j\neq(r-1)/2,j=1}^{L}Z_{2j-1}Z_{2j+1}}, \end{aligned} \tag{32}$$

while the one with no Z_2 symmetry is

$$\begin{aligned} T_{\sigma,A} = &e^{-i(J_xT/2)\sum_{j=1}^{L}X_{2j-1}X_{2j+1}} \\ &\times e^{-i(gT/2)\sum_{j\neq(r-1)/2,j=1}^{L}X_{2j+1}} \\ &\times e^{-i(JT/2)Z_{r-2}X_r}e^{-i(JT/2)\sum_{j\neq(r-1)/2,j=1}^{L}Z_{2j-1}Z_{2j+1}}. \end{aligned} \tag{33}$$

Above, site $2L+1$ is identified with site 1 and so an exchange term of the kind $Z_{2L-1}Z_{2L+1}$ is the same as $Z_{2L-1}Z_1$,

and the exchange term $X_{2L-1}X_{2L+1}$ is the same as $X_{2L-1}X_1$. J_x parametrizes the strength of the integrability breaking interactions.

Let us define an infinite-temperature autocorrelation function of the Pauli spins Y_r, Z_r at site r at stroboscopic time n as

$$A^{Y_r}_{\infty}(n) = \frac{1}{2^L}\mathrm{Tr}[Y_r(n)Y_r(0)], \tag{34}$$

$$A^{Z_r}_{\infty}(n) = \frac{1}{2^L}\mathrm{Tr}[Z_r(n)Z_r(0)]. \tag{35}$$

It is Y_r that has an overlap with the Majorana zero mode in the integrable limit of $J_x = 0$, and therefore stability of the zero mode will be explored by the study of $A^{Y_r}_{\infty}$. In addition, the left-out Majorana in the integrable limit is identical to Z_r, and therefore its unusual dynamics, even in the integrable case, will be explored through the study of $A^{Z_r}_{\infty}$.

We also find it helpful to construct a numerical conserved quantity with an overlap with Y_r,

$$Q = \sum_{\beta} \langle\beta|Y_r|\beta\rangle|\beta\rangle\langle\beta|, \tag{36}$$

where $|\beta\rangle$ denote the exact eigenstates of $T_{\sigma,S/A}$. Then, we expect that if such a conserved quantity exists, the plateau height of the autocorrelation function of Y_r will be given by

$$P = \langle Q^2\rangle = \frac{1}{2^L}\sum_{\beta} |\langle\beta|Y_r|\beta\rangle|^2, \tag{37}$$

with $P = \lim_{n\to\infty} A^{Y_r}_{\infty}(n)$. We will plot the corresponding P along with the autocorrelation function.

For the rest of the paper, we take $JT/2 = 1.0, T = 2.0$ while considering different g and J_x. To orient oneself, let us first consider the integrable case of $J_x = 0$. Figure 2 shows $A^{Y_r}_{\infty}$ for chains of different lengths and $gT/2 = 0.3$. The plot shows that this autocorrelation function does not decay with time. The horizontal gray line is the value of P in (37). Unlike the $J_x \neq 0$ cases discussed later, P is not L dependent for the integrable case of $J_x = 0$. Figure 3 shows $A^{Z_r}_{\infty}$ for the same parameters and shows that this decays within time of $O(1)$. This rapid decay can be interpreted as rapid decoherence due to x-ray edge-type processes [see (29)] or, equivalently, due to the nonlocal string correlation described by (28), building up over time.

We now break integrability by including four-fermion interactions. Our goal is to explore the fate of the Majorana zero mode. Figure 4 presents results for $JT/2 = 1.0, T = 2.0, g = 0.3, J_x = 0.1$ for the Z_2 symmetry-breaking case and for different system sizes. After an initial transient, $A^{Y_r}_{\infty}$ settles into a plateau. The height of the plateau decreases as L increases, and agrees very well with the quantity P as defined in (37), which is related to the conserved quantity Q. While plateau heights in Fig. 4 depend on L, the n dependence of the correlation function before the plateau is reached does not depend on L. It fits an exponential very well for the chosen parameters. This exponential can be used to extract a decay rate.

The decay rates for several different J_x and for $JT/2 = 1.0, T = 2.0, g = 0.3$ are plotted in Fig. 5. The decay rates indicate a J_x^2 dependence, a result also expected

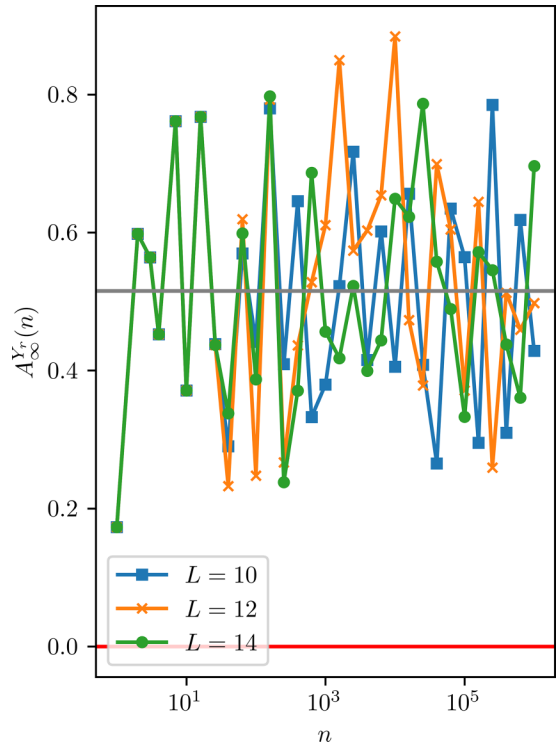

FIG. 2. Autocorrelation function (34) where Y_r has an overlap with the Majorana zero mode, and for the integrable case $J_x = 0$. The other parameters are $gT/2 = 0.3, JT/2 = 1.0$. Gray lines are the numerically constructed plateau heights P (37) related to the conserved quantity Q (36). When $J_x = 0$, P shows little dependence on L.

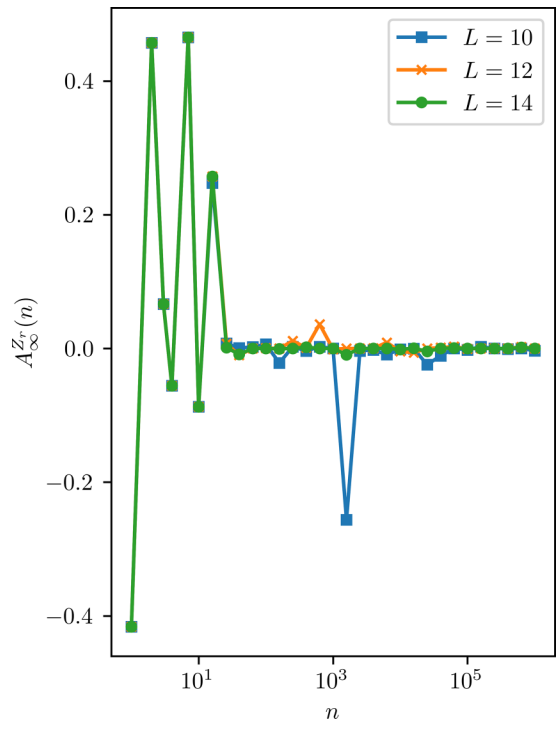

FIG. 3. Autocorrelation function (35) where $Z_r = \gamma_{2L-2}$. This is the Majorana operator that is left out of the integrable Floquet unitary with $J_x = 0$. The other parameters are $gT/2 = 0.3, JT/2 = 1.0$.

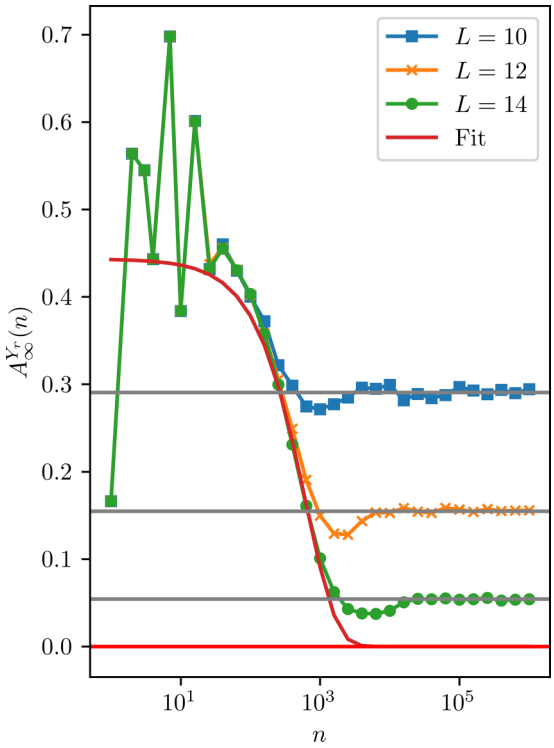

FIG. 4. The autocorrelation function (34) for the nonintegrable case where $gT/2 = 0.3, JT/2 = 1.0, T = 2.0, J_x = 0.1$, and there is no Z_2 symmetry. Plateaus agree well with the gray lines which are the numerically constructed plateau heights P, related to the conserved quantity Q. The red line is a fit to an exponential decay $\sim \exp(-\text{decay rate}\, n)$.

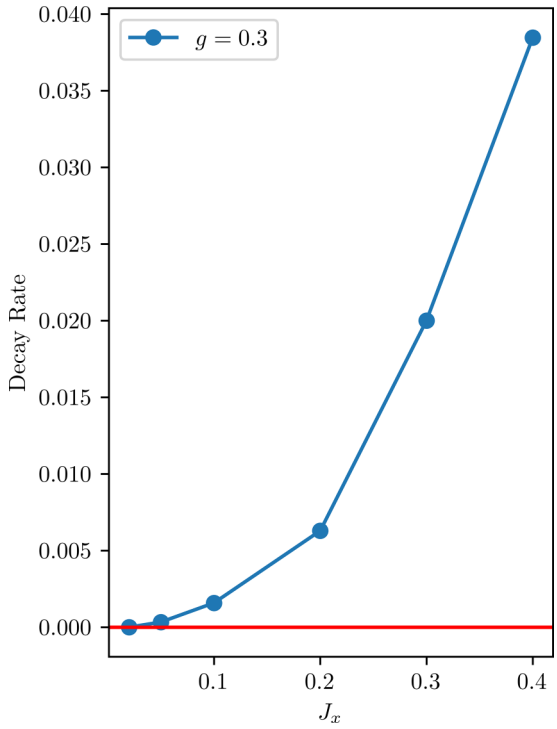

FIG. 5. Decay rates for different J_x for $JT/2 = 1.0$, T=2.0, $gT/2$=0.3, and no Z_2 symmetry. Decay rates are obtained from fitting the approach to the plateau to an exponential. The decay rates approximately grow with J_x^2 for the chosen parameters.

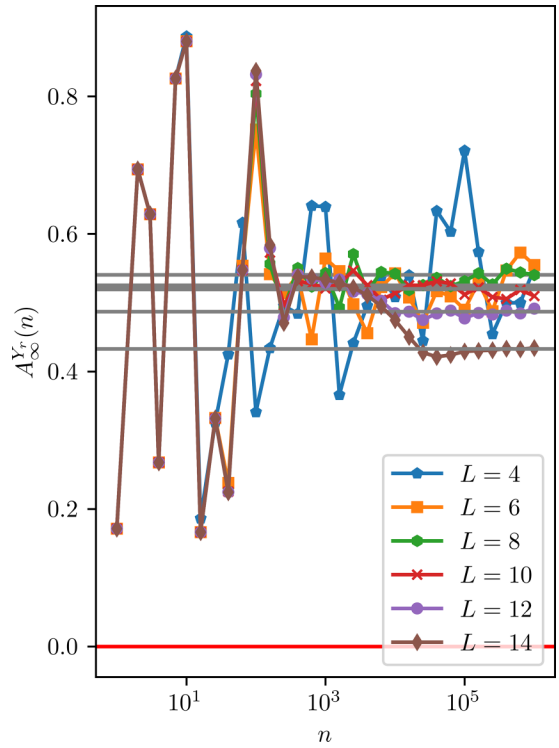

FIG. 6. Autocorrelation function for $JT/2 = 1.0$, $T = 2.0, gT/2 = 0.1$, $J_x = 0.05$ and no Z_2 symmetry. Plateaus agree well with the gray lines which are the numerically constructed plateau heights P, related to the conserved quantity Q. Smaller transverse fields g and interactions J_x require a larger system size L for seeing a significant drop in the plateau height (compare with Fig. 4).

from applying Fermi's Golden Rule for the above values of $gT/2, JT/2$ [23].

Quite generally, if we make the integrability breaking term smaller and/or the Majorana mode too localized [for example, by reducing the ratio of $\min(g, J)/\max(g, J)$], the system sizes needed to observe a significant decrease in the plateau heights become too large. This is demonstrated in Figs. 6 and 7, which are both for $gT/2 = 0.1, JT/2 = 1.0, T = 2.0, J_x = 0.05$, but with the former figure for the case with no Z_2 symmetry, while the latter for the case with Z_2 symmetry. We observe the same qualitative behavior for the two cases.

It is interesting to note that for the integrable case (Fig. 2), although the plateaus are L independent, the autocorrelation function fluctuates about the plateau considerably. This is because when the system is integrable, Y_{2L-1} has overlap not just with the Majorana zero mode, but also with other conserved quantities, such as delocalized quasiparticles. The latter oscillates, causing an oscillatory behavior of the plateau controlled by the single-particle level spacing, proportional to $1/L$. When interactions are included, these delocalized quasiparticles are not conserved, causing the oscillations to dampen rapidly, leaving only the effect of a single conserved quantity Q and tiny oscillations arising from the exponentially small many-particle level spacing. This is the reason why the oscillations about the plateau value are absent in Fig. 4.

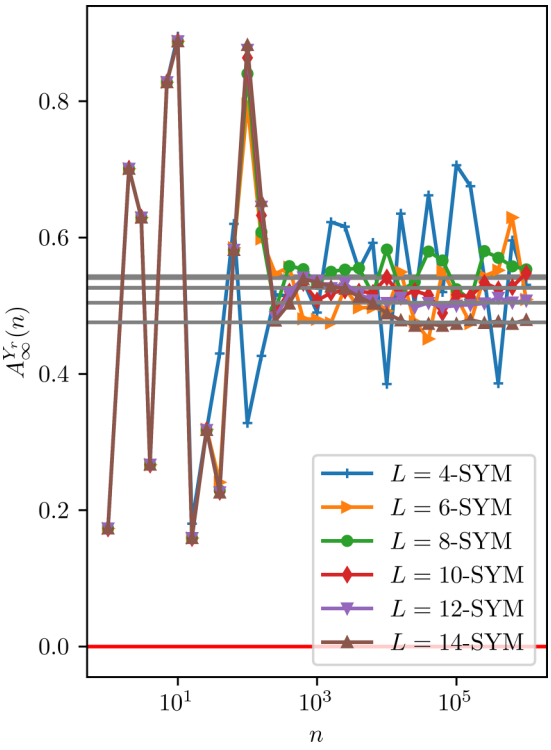

FIG. 7. Autocorrelation function for $gT/2$=0.1, $JT/2$=1.0, $T = 2.0$, $J_x = 0.05$ and with Z_2 symmetry. Plateaus agree well with the gray lines which are the numerically constructed plateau heights P, related to the conserved quantity Q. No qualitative difference is observed between the cases with and without Z_2 symmetry, where P is slightly larger for the former case in comparison to the latter case (Fig. 6), for the same parameters.

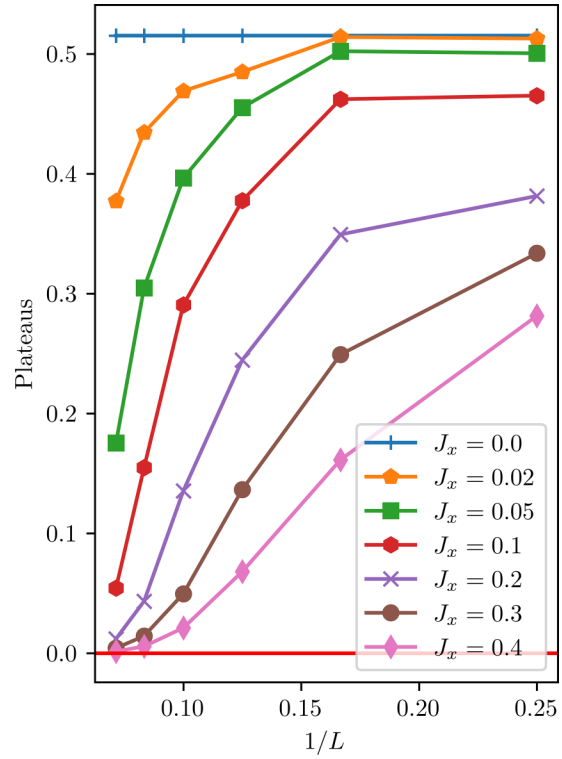

FIG. 8. Plateau heights P (37) vs $1/L$ for different J_x for the case where there is no Z_2 symmetry and $JT/2 = 1.0$, $T = 2.0$, $gT/2 = 0.3$.

IV. PLATEAU HEIGHT AND FOCK-SPACE DELOCALIZATION

Figure 8 plots the plateau heights P as a function of system size L for the case of no Z_2 symmetry, for several different g, J_x, with $JT/2 = 1.0$, $T = 2.0$. The plateau height is a finite system size effect because as $L \to \infty$, $P \to 0$. A generic nonintegrable interacting many-particle system at finite or, as in our case, infinite temperature is ergodic and equilibrates if it is sufficiently large [24–32]. The nature of the eigenstates of the time-evolution operator changes dramatically as a function of J_x. For $J_x = 0$, eigenstates are simple many-particle Fock states $|\Omega, \vec{n}\rangle$, parameterized by $\Omega = \pm 1$ and the occupation numbers n_i, $i = 1, \ldots, L-1$ of the fermionic modes of the system. Using this notation, one can identify the Majorana zero mode Ψ with the parity of the bulk states, $\Psi|\Omega, \vec{n}\rangle = (-1)^{\sum_i n_i}|\Omega, \vec{n}\rangle$. Interactions can be viewed as inducing a hopping process from one Fock state to a neighboring one with a different energy and thus equilibration by interactions can be viewed as a delocalization process in Fock space, as has been shown in the seminal work of Altshuler *et al.* [33] on interacting chaotic quantum dots.

When wave functions are localized in Fock space, the Majorana zero mode will not decay and the plateau value of the Y_r autocorrelation function, given by Eq. (37), is a number of the order of 1. In contrast, in the fully Fock-space delocalized phase, a typical eigenstate will have the form $|\Psi_{\rm typ}\rangle = \sum_{\vec{n},\Omega} a_{\Omega\vec{n}}|\Omega, \vec{n}\rangle$ with $|a_{\Omega\vec{n}}| \sim 1/\sqrt{2^L}$, and the plateau value will be roughly

$$\begin{aligned} P_{\text{Fock-delocalized}} &\sim |\langle\Psi_{\rm typ}|Y_r|\Psi_{\rm typ}\rangle|^2 \\ &= \left|\sum_{\Omega,\vec{n},\vec{m}} a^*_{\Omega\vec{n}} a_{\Omega\vec{m}} \langle\Omega, \vec{n}|Y_r|\Omega, \vec{m}\rangle\right|^2 \\ &\sim \left|\frac{c}{2^L}\sum_{\vec{n}}(\pm 1)\right|^2 \sim \frac{1}{2^L}, \end{aligned} \tag{38}$$

where we used that Y_r and the Majorana mode Ψ have a finite overlap, $Y_r \sim c\Psi$, that Ψ has eigenvalues ± 1, and that the sum of $N = 2^L$ numbers of the order of 1 with random signs is of the order of $\sqrt{N}$. The value of the plateau which we observe numerically for small J_x and L is, however, much larger than that predicted by (38). A sizable plateau thus implies that the wave function remains at least partially localized in Fock space. In this case, the sum in (38) runs only over a small number of terms, giving rise to large plateau values. The quantitative link of localization and size of the plateau is discussed numerically below.

To understand how J_x induces a delocalization transition in a finite-size system, we need to consider three types of matrix elements of the interactions, $M_{\rm eM}$, $M_{\rm ee}$, and $M^b_{\rm ee}$. These describe the scattering of the boundary Majorana with three extended bulk states $M_{\rm eM}$, the momentum-conserving scattering of four extended bulk states $M_{\rm ee}$, and the scattering of four extended bulk states at the boundary without momentum conservation $M^b_{\rm ee}$.

A bulk state with momentum k has a single-particle wave function of the form $\exp(ikR_j)/\sqrt{L}$, where R_j denotes the particle position. Thus a typical four-Majorana bulk-interaction matrix element in a clean system scales with $(J_x/\sqrt{L}^4)\sum_j \exp[i(k_1+k_2+k_3+k_4)R_j] = (J_xL/\sqrt{L}^4)\delta_{k_1+k_2+k_3+k_4,0}$. Each k has L possible values and there are therefore L^3 possible combinations of k_i fulfilling momentum conservation. Thus bulk interactions connect a given Fock state to $Z_{\rm ee} = L^3$ other Fock states with a matrix element $M_{\rm ee}$ of the order of $J_xL/\sqrt{L}^4$.

We can repeat this argument for boundary scattering of extended bulk states. In this case, the matrix element is suppressed by a factor $1/L$, $M^b_{\rm ee} \sim M_{\rm ee}/L$, but, due to the absence of momentum conservation, the number of connecting neighbors in Fock space increases, $Z^b_{\rm ee} \sim Z_{\rm ee}L$.

Finally, the matrix element of a localized Majorana mode with wave function ϕ_j interacting with three delocalized bulk modes scales with $(J_x/\sqrt{L}^3)\sum_j \phi_j \exp[i(k_1+k_2+k_3)R_j] \sim J_x/\sqrt{L}^3$, giving rise to a hopping to $Z_{\rm eM} \sim L^3$ neighbors in Fock space.

Thus, we have found the following scaling with system size L:

$$\begin{aligned} M_{\rm eM} &\sim \frac{J_x}{(\sqrt{L})^3}, \quad Z_{\rm eM} \sim L^3, \\ M_{\rm ee} &\sim \frac{J_xL}{(\sqrt{L})^4} = \frac{J_x}{L}, \quad Z_{\rm ee} \sim L^3, \\ M^b_{\rm ee} &\sim \frac{J_x}{(\sqrt{L})^4}, \quad Z^b_{\rm ee} \sim L^4. \end{aligned} \tag{39}$$

Note that the $M_{\rm ee}$ and $M^b_{\rm ee}$ processes conserve the edge Majorana Ψ or, equivalently, the parity of bulk states $(-1)^{\sum_i n_i}$, while the $M_{\rm eM}$ processes flip Ψ. At least locally [33], the interaction-induced scattering leads to a hopping problem on a Cayley tree [34] with a large coordination number, as sketched in Fig. 9.

Importantly, the Fock states connected by the above-described matrix elements typically have very different quasienergies (defined modulo $2\pi/T$). This difference of quasienergies of states connected by J_x depends on the chosen parameters. For the following discussion, we focus on a regime where $gT/2$ and $JT/2$ are both numbers of the order of 1 and where, in the thermodynamic limit, the Majorana zero mode is in the middle of a continuum spanned by the sums and differences of three bulk-state quasienergies, ϵ_k, i.e., one can find solutions for $\epsilon_{k_1} \pm \epsilon_{k_2} \pm \epsilon_{k_3} = 2\pi n/T$, $n \in \mathbb{Z}$, in the thermodynamic limit. A straightforward Fermi's Golden Rule argument [23] predicts that in this case, the inverse lifetime of the Majorana scales with J_x^2, which is, e.g., fulfilled for the parameters chosen in Fig. 5. Under these conditions, the typical differences of quasienergies of Fock states connected by J_x is of the order of $E_0 \sim J \sim g \sim 2\pi/T$. If a given Fock state has Z neighbors, the typical minimal energy difference is thus E_0/Z. Thus, one can obtain a first estimate of the delocalization transition by comparing M_α to E_0/Z_α, where α labels the particular scattering process in (39). More precisely, it has been shown by Abou-Chacra *et al.* [34] that for large Z and on a Cayley tree, the system starts to delocalize in Fock space for

$$M_\alpha \gtrsim \frac{E_0}{Z_\alpha \ln[Z_\alpha]}. \tag{40}$$

Note that the applicability of this formula for interaction-induced delocalization in Fock space has been controversial even for the most intensively studied problem of a chaotic interacting quantum dot (see Ref. [35] for a discussion of arguments and publications pointing to different dependencies on Z_α), but large parts of the recent literature seem to agree with Eq. (40); see e.g., [32,36]. Our numerical results are at least consistent with (40) and we will use (40) only for qualitative arguments below.

Using (40) for the processes of (39) reveals that upon increasing J_x starting from the noninteracting system, the delocalization of Fock states occurs first via the two bulk-mode scattering processes $M_{\rm ee}$ and $M^b_{\rm ee}$ at $J_x \sim E_0/L^2$ if we ignore logarithmic corrections. While $M^b_{\rm ee} \ll M_{\rm ee}$, it profits from a larger number of accessible states such that $M_{\rm ee}Z_{\rm ee} \sim M^b_{\rm ee}Z^b_{\rm ee}$. As nominally $\ln Z^b_{\rm ee} > \ln Z_{\rm ee}$, Eq. (40) strictly speaking predicts that $M^b_{\rm ee}$ is more important than $M_{\rm ee}$ for very large systems.

For our discussion, another effect is more important. Due to delocalization, one obtains an effective broadening of the

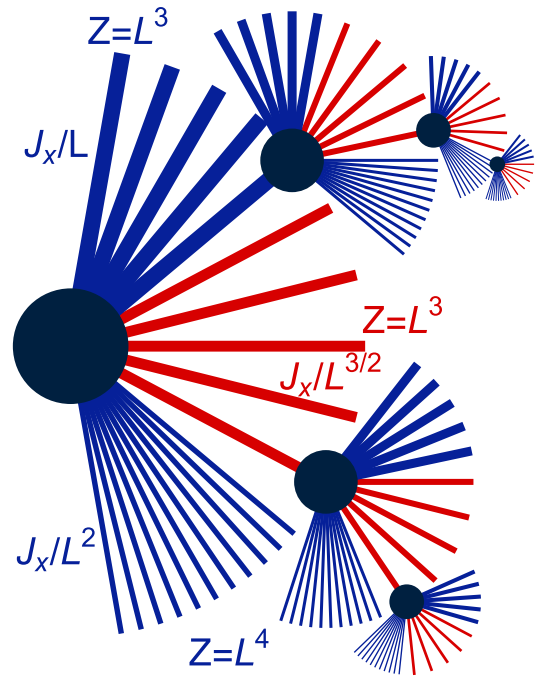

FIG. 9. Interactions J_x induce a hopping from one of the 2^L Fock-space states (black dots) to the next, if they are connected by a four-Majorana process. Thick blue lines: momentum-conserving scattering processes of extended bulk states with matrix element $M_{\rm ee} \sim J_x/L$. $Z = L^3$ is the number of neighboring states connected by this process. Thin blue lines: scattering of extended states without momentum conservation, $M^b_{\rm ee} \sim J_x/L^2$. Red lines: interaction terms involving the Majorana zero mode at the boundary/twist, $M_{\rm eM} \sim J_x/L^{3/2}$. For $J_x \ll J/L^2$, Fock states remain localized, but upon increasing J_x, bulk scattering leads to a delocalization in Fock space, followed by an activation of edge-Majorana scattering events.

quasienergies of the Fock states at $M_\alpha \sim E_0/Z_\alpha$ (ignoring, again, logarithms), of the order of E_0/Z_α [36] with $E_0/Z_{ee} \gg E_0/Z^b_{ee}$. Thus, the broadening of Fock levels is dominated by the momentum-conserving bulk-scattering processes, as we show numerically below.

This leads to the following physical picture upon increasing J_x in a finite-size system: first, Fock-space hopping induces a delocalization in Fock space at a small value of the coupling, $J_x \sim E_0/L^2$. This delocalization induces a broadening of the quasienergies of Fock states, mainly driven by bulk-scattering processes shown as thick blue lines in Fig. 9. This broadening effectively unblocks scattering processes involving the localized Majorana mode at the boundary for slightly larger J_x. Due to the "unblocking," the plateau in the Y_r correlation function decays. We would like to stress that this analysis only applies to the case of a *single* zero-energy Majorana mode, which is the focus of this study. In the presence of several zero-energy modes, there are extra degeneracies in the many-particle spectrum of the noninteracting system, which have to be taken into account separately.

To corroborate this picture numerically, we will show, in the following, (i) that the delocalization of bulk states in Fock space is governed by bulk-scattering processes and (ii) that the localization/delocalization of Fock states governs the formation/decay of the plateau of the Majorana correlation function.

Denoting $|\beta_0\rangle$ as an eigenstate of the integrable system or, equivalently, a Fock state, our goal is to study the fate of the bulk conserved quantity $|\beta_0\rangle\langle\beta_0|$ when integrability-breaking interactions are switched on. The infinite-temperature autocorrelation function of this quantity is $|\langle\beta_0|T^n_{\sigma,S/A}|\beta_0\rangle|^2$. We can also interpret this quantity as the return probability that the quantum system starting in the Fock state $|\beta_0\rangle$ is still in the same Fock state after n time steps. Averaging the return probability over all conserved quantities gives

$$\begin{aligned}&\text{Average return probability}(n)\\ &= \frac{1}{2^L}\sum_{\beta_0} |\langle\beta_0|T^n_{\sigma,S/A}|\beta_0\rangle|^2\\ &= \frac{1}{2^L}\sum_{\beta_0,\beta,\beta'} |\langle\beta_0|\beta\rangle|^2|\langle\beta'|\beta_0\rangle|^2 e^{-i(\epsilon_\beta-\epsilon_{\beta'})Tn}. \end{aligned} \tag{41}$$

Above, ϵ_β denote the quasienergy associated with the eigenstate $|\beta\rangle$ of the nonintegrable unitary $T_{\sigma,S/A}$. In (41), we use the Fock states of the integrable model, $J_x = 0$, thus neglecting the effect that Fock states will obtain Hartree-Fock-style corrections from J_x which may lead to a suppression of Fock state overlaps $\sim \exp[-\text{const}\,(J_x/E_0)^2 L]$. Neglecting this is justified even for large L, as typical values of J_x triggering Fock space delocalization are tiny, $J_x \sim E_0/L^2$, according to (40); see, also, Fig. 11 below.

The average return probability is plotted in Fig. 10 for the same parameters as Fig. 4. The gray lines correspond to taking the long-time limit where one may project onto the diagonal ensemble, $\beta = \beta'$. In this limit, the average return probability equals the inverse participation ratio (IPR) in Fock space,

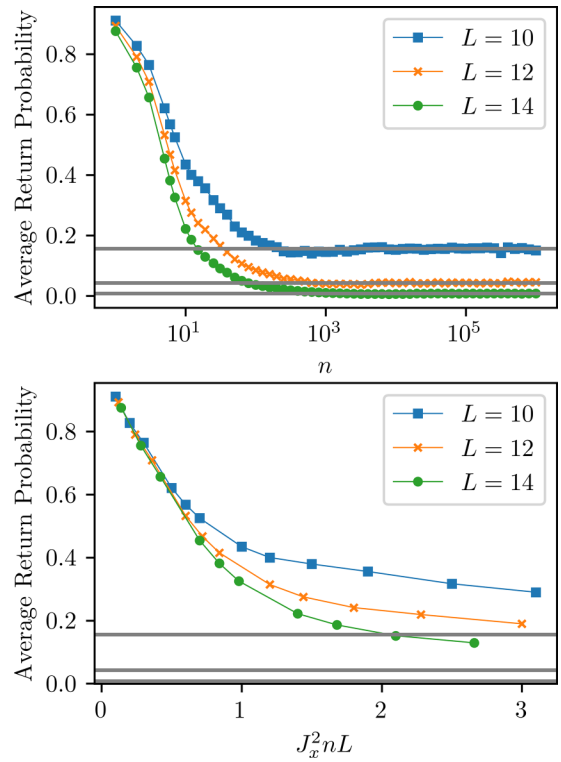

FIG. 10. Top panel: Average return probability vs stroboscopic time n. After an initial transient, this quantity approaches a plateau whose magnitude agrees well with the IPR, the latter indicated by the gray lines. Bottom panel: Same as top panel, but now plotted vs $J_x^2 nL$. The parameters for both panels are $JT/2 = 1.0$, $T = 2.0$, $gT/2 = 0.3$ and $J_x = 0.1$, with no Z_2 symmetry.

$$\begin{aligned}&\text{Average return probability}(n \to \infty)\\ &= \text{IPR} = \frac{1}{2^L}\sum_{\beta_0,\beta} |\langle\beta_0|\beta\rangle|^4. \end{aligned} \tag{42}$$

The IPR is a common measure of delocalization: a wave function delocalized over roughly N states (here, in Fock space) has $|\langle\beta_0|\beta\rangle|^2 \sim 1/N$ for N states $|\beta\rangle$, resulting in an IPR of the order of $N/N^2 = 1/N$, with $N \sim 2^L$ in the fully delocalized limit.

The Fermi's Golden Rule formula suggests that the inverse lifetime of a typical Fock state $|\beta\rangle$ in the delocalized phase (or for short times, see below) scales as $2\pi\sum_{\beta'} |\langle\beta'|H_{\text{int}}|\beta\rangle|^2\delta(\epsilon_\beta - \epsilon'_\beta) \sim \sum_\alpha \Gamma_\alpha$ with $\Gamma_\alpha \sim |M_\alpha|^2 Z_\alpha/E_0$, where we sum over all possible bulk, edge, and Majorana scattering channels α and assume that the effective broadening of the δ function is larger than the effective level spacing of neighboring states in Fock space, E_0/Z_α. Using (39), the shortest lifetime arises from bulk-scattering processes with $\Gamma_{ee} \sim |M_{ee}|^2 Z_{ee}/E_0 \sim L J_x^2/E_0$. In contrast, the boundary scattering processes with and without the Majorana mode give $\Gamma_{em} \sim \Gamma^b_{ee} \sim J_x^2/E_0 \ll \Gamma_{ee}$ and can therefore be neglected. Thus, we plot in Fig. 10 (lower panel) the average return probability as a function of $J_x^2 nL$. For short times, we obtain an excellent collapse and the larger the system, the longer it follows the expected exponential decay on a

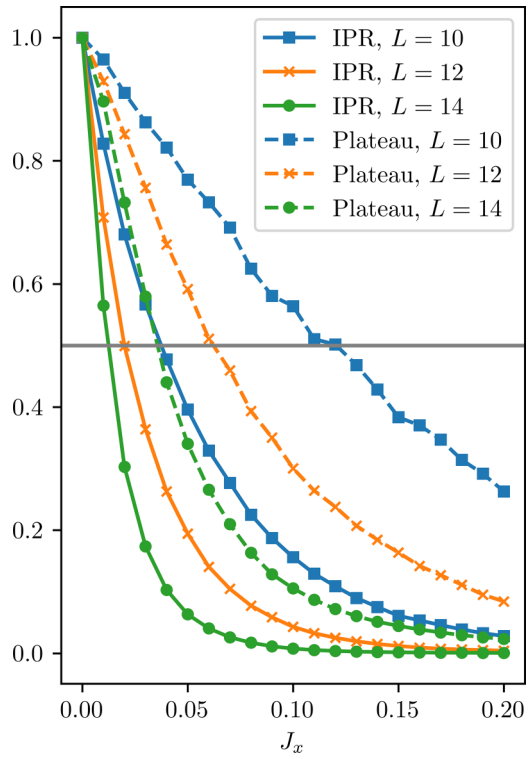

FIG. 11. IPR and normalized plateau heights $P(J_x)/P(J_x = 0)$ vs J_x for the case where there is no Z_2 symmetry and $JT/2 = 1.0$, $T = 2.0$, $g = 0.3$.

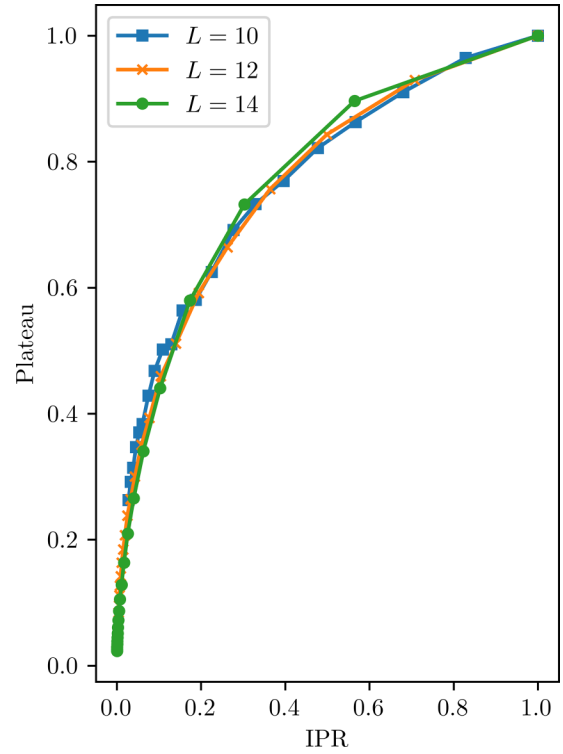

FIG. 12. Normalized plateau $P(J_x)/P(J_x = 0)$ vs IPR for the case where there is no Z_2 symmetry and $JT/2 = 1.0$, $T = 2.0$, $g = 0.3$.

timescale of the order of $1/\Gamma_{ee}$. This indicates that bulk scattering is—as expected—the dominant decay mechanism of Fock states. The plateau obtained for larger times and small systems, which we identified with the IPR, implies that the wave functions remain partially localized in Fock space. Delocalization is expected to occur when the broadening of Fock levels, Γ_{ee}, becomes larger than the relevant level spacing, $\Gamma_{ee} \gtrsim E_0/Z_{ee}$, or, equivalently, $M_{ee} \gtrsim E_0/Z_{ee}$. This condition is (up to the logarithm not covered by this simple argument) consistent with (40).

After we have established that the delocalization in Fock space is governed by bulk-scattering processes, we will now show that this delocalization also governs the destruction of the plateau of the Majorana correlation function. Figure 11 plots, for three different system sizes, both the plateau heights and the average Fock space IPR, which is used to keep track of delocalization in Fock space (see discussion above), as a function of the interaction strength J_x. As expected, both quantities vanish for large J_x when the system becomes ergodic. For larger systems, smaller values of J_x are sufficient to induce both delocalization and a suppression of the plateau. To show that these two processes, delocalization by bulk scattering and decay of the Majorana mode, are directly linked with each other, we plot in Fig. 12 the (normalized) plateau value as a function of the IPR, using the data of Fig. 11. Remarkably, different system sizes now approximately collapse on a single curve. It is a surprising numerical observation that the plateau height as a function of the IPR appears to depend only weakly on system size. The figure is fully consistent with our theoretical scenario that the delocalization in Fock space, measured by the reduction of the IPR, activates edge-Majorana scattering and therefore suppresses the plateau in the edge-correlation function. In our example, the plateau is reduced to roughly half of its size when the IPR is 0.1, implying a delocalization in Fock space covering roughly 10 Fock states.

V. CONCLUSIONS

Interacting Floquet systems are a bedrock for studying nonequilibrium and topological phenomena, where the latter are sensitive to boundary conditions. In this paper, we have explored the role of a special boundary condition, i.e., the duality twisted boundary condition on these systems. The role of the duality twist was to introduce a single Majorana zero mode in an integrable Floquet unitary, for all coupling parameters of the unitary. In addition, this isolated Majorana zero mode did not lead to any degeneracies of the Floquet eigenspectra. This is quite unlike open boundary conditions where the Majorana zero modes appear in pairs, which arise for special couplings (transverse fields smaller than Ising interactions), and cause a degeneracy of the Floquet spectra. We showed that even though for spatially uniform transverse fields and Ising couplings, the Majorana zero mode is localized at the duality twist, this is actually a special limit where a domain wall is absent. In particular, a unitary transformation can be performed that moves the duality twist relative to the Majorana zero mode, with the Majorana zero mode now residing at a domain wall separating two regions that are related by the interchange of the Ising couplings and the transverse-field couplings.

We studied the effect of interactions for the case where the Majorana zero mode resides near the duality twist, i.e., in the absence of a domain wall. While the Majorana zero mode does not survive in the thermodynamic limit when interactions are nonzero, nevertheless, we found that for finite system sizes, the Majorana zero mode is related to an emergent symmetry. The signature of this was an autocorrelation function which, after an initial transient, approached a plateau. The height of the plateau was found to agree very well with a numerically constructed conserved quantity which overlaps with the integrable Majorana zero mode. These results were quite insensitive to whether or not the interactions preserved the Z_2 symmetry, with differences appearing only in details such as the precise values of the plateau heights.

A theory was presented for the eventual decay of the plateau in the thermodynamic limit in the language of Fock space delocalization [32]. In the absence of interactions, the conserved quantities, both boundary and bulk, are localized in Fock space. Once interactions are switched on, hopping in Fock space sets in, but for very small interactions the many-particle wave functions remain localized in Fock space. We showed that the matrix elements for decay of the bulk conserved quantities are larger than the boundary conserved quantity. Thus, as the interactions are increased, the wave function starts to delocalize in Fock space and bulk conserved quantities decay first, followed by the boundary conserved quantity. This phenomena was supported by ED, which showed that the average autocorrelation function of all bulk conserved quantities reached a steady state at earlier stroboscopic times than the boundary autocorrelation function, where the steady-state value of the former is the IPR. In addition, we showed that the IPR decay directly controls the decay of the plateau height associated with the boundary Majorana mode. We expect that the physics of a multistep localization/delocalization transition will also have applications for other integrable systems subject to weak integrability-breaking perturbations.

There are many open questions. Generalizing the study of the physics of duality twisted boundary conditions to other systems, such as Z_N spin chains, is an obvious direction of study. Further, the role of more than one topological defect on the dynamics of the system is an interesting direction of research.

ACKNOWLEDGMENTS

The authors are deeply indebted to Alex Altland and Dries Sels for many helpful discussions. This work was supported by the US National Science Foundation under Grant No. NSF-DMR 2018358 (A.M.), in part by the US National Science Foundation under Grant No. NSF PHY-1748958 (A.M.), and by the German Research Foundation within CRC183 [Project No. 277101999, subproject A01 (A.R.) and a Mercator fellowship (A.M.)].

[1] H. A. Kramers and G. H. Wannier, Statistics of the two-dimensional ferromagnet. Part I, Phys. Rev. **60**, 252 (1941).

[2] D. Aasen, R. S. K. Mong, and P. Fendley, Topological defects on the lattice: I. the Ising model, J. Phys. A: Math. Theor. **49**, 354001 (2016).

[3] D. Aasen, P. Fendley, and R. S. Mong, Topological defects on the lattice: Dualities and degeneracies, arXiv:2008.08598.

[4] L. Lootens, C. Delcamp, G. Ortiz, and F. Verstraete, Dualities in one-dimensional quantum lattice models: Symmetric Hamiltonians and matrix product operator intertwiners, arXiv:2112.09091.

[5] E. P. Verlinde, Fusion rules and modular transformations in 2D conformal field theory, Nucl. Phys. B **300**, 360 (1988).

[6] J. L. Cardy, Boundary conditions, fusion rules and the Verlinde formula, Nucl. Phys. B **324**, 581 (1989).

[7] V. B. Petkova and J. B. Zuber, Generalized twisted partition functions, Phys. Lett. B **504**, 157 (2001).

[8] J. Fröhlich, J. Fuchs, I. Runkel, and C. Schweigert, Kramers-Wannier Duality from Conformal Defects, Phys. Rev. Lett. **93**, 070601 (2004).

[9] C.-M. Chang, Y.-H. Lin, S.-H. Shao, Y. Wang, and X. Yin, Topological defect lines and renormalization group flows in two dimensions, J. High Energy Phys. 01 (2019) 026.

[10] M. T. Tan, Y. Wang, and A. Mitra, Topological defects in floquet circuits, arXiv:2206.06272.

[11] N. Tantivasadakarn, R. Thorngren, A. Vishwanath, and R. Verresen, Long-range entanglement from measuring symmetry-protected topological phases, arXiv:2112.01519.

[12] D. Aasen, Z. Wang, and M. B. Hastings, Adiabatic paths of Hamiltonians, symmetries of topological order, and automorphism codes, Phys. Rev. B **106**, 085122 (2022).

[13] D. Levy, Algebraic Structure of Translation-Invariant Spin-1/2 *XXZ* and q-Potts Quantum Chains, Phys. Rev. Lett. **67**, 1971 (1991).

[14] U. Grimm and G. Schutz, The spin-1/2 *XXZ* Heisenberg chain, the quantum algebra $u_q[sl(2)]$, and duality transformations for minimal models, J. Stat. Phys. **71**, 923 (1993).

[15] M. Oshikawa and I. Affleck, Boundary conformal field theory approach to the critical two-dimensional Ising model with a defect line, Nucl. Phys. B **495**, 533 (1997).

[16] C. Chui, C. Mercat, W. P. Orrick, and P. A. Pearce, Integrable lattice realizations of conformal twisted boundary conditions, Phys. Lett. B **517**, 429 (2001).

[17] U. Grimm, Spectrum of a duality twisted Ising quantum chain, J. Phys. A: Math. Gen. **35**, L25 (2002).

[18] A. Roy and H. Saleur, Entanglement entropy in critical quantum spin chains with boundaries and defects, arXiv:2111.07927.

[19] P. Fendley, Strong zero modes and eigenstate phase transitions in the *XYZ*/interacting Majorana chain, J. Phys. A: Math. Theor. **49**, 30LT01 (2016).

[20] M. Thakurathi, A. A. Patel, D. Sen, and A. Dutta, Floquet generation of Majorana end modes and topological invariants, Phys. Rev. B **88**, 155133 (2013).

[21] D. J. Yates, F. H. L. Essler, and A. Mitra, Almost strong $(0, \pi)$ edge modes in clean interacting one-dimensional Floquet systems, Phys. Rev. B **99**, 205419 (2019).

[22] M. Hauru, G. Evenbly, W. W. Ho, D. Gaiotto, and G. Vidal, Topological conformal defects with tensor networks, Phys. Rev. B **94**, 115125 (2016).
[23] H.-C. Yeh, A. Rosch, and A. Mitra, Decay rates of almost strong modes in Floquet spin chains beyond Fermi's golden rule, arXiv:2305.04980.
[24] D. A. Rabson, B. N. Narozhny, and A. J. Millis, Crossover from poisson to Wigner-Dyson level statistics in spin chains with integrability breaking, Phys. Rev. B **69**, 054403 (2004).
[25] P. Jung, R. W. Helmes, and A. Rosch, Transport in Almost Integrable Models: Perturbed Heisenberg Chains, Phys. Rev. Lett. **96**, 067202 (2006).
[26] P. Jung and A. Rosch, Spin conductivity in almost integrable spin chains, Phys. Rev. B **76**, 245108 (2007).
[27] M. Rigol, V. Dunjko, and M. Olshanii, Thermalization and its mechanism for generic isolated quantum systems, Nature (London) **452**, 854 (2008).
[28] L. F. Santos and M. Rigol, Onset of quantum chaos in one-dimensional bosonic and fermionic systems and its relation to thermalization, Phys. Rev. E **81**, 036206 (2010).
[29] M. Tavora, A. Rosch, and A. Mitra, Quench Dynamics of One-Dimensional Interacting Bosons in a Disordered Potential: Elastic Dephasing and Critical Speeding-Up of Thermalization, Phys. Rev. Lett. **113**, 010601 (2014).
[30] A. Mitra, Quantum quench dynamics, Annu. Rev. Condens. Matter Phys. **9**, 245 (2018).
[31] M. Žnidarič, Weak Integrability Breaking: Chaos with Integrability Signature in Coherent Diffusion, Phys. Rev. Lett. **125**, 180605 (2020).
[32] V. B. Bulchandani, D. A. Huse, and S. Gopalakrishnan, Onset of many-body quantum chaos due to breaking integrability, Phys. Rev. B **105**, 214308 (2022).
[33] B. L. Altshuler, Y. Gefen, A. Kamenev, and L. S. Levitov, Quasiparticle Lifetime in a Finite System: A Nonperturbative Approach, Phys. Rev. Lett. **78**, 2803 (1997).
[34] R. Abou-Chacra, D. J. Thouless, and P. W. Anderson, A self-consistent theory of localization, J. Phys. C **6**, 1734 (1973).
[35] I. V. Gornyi, A. D. Mirlin, and D. G. Polyakov, Many-body delocalization transition and relaxation in a quantum dot, Phys. Rev. B **93**, 125419 (2016).
[36] F. Monteiro, M. Tezuka, A. Altland, D. A. Huse, and T. Micklitz, Quantum Ergodicity in the Many-Body Localization Problem, Phys. Rev. Lett. **127**, 030601 (2021).